Adıyaman University Journal of Science
https://dergipark.org.tr/en/pub/adyujsci
DergiPark AKADEMİK
ISSN 2147-1630
e-ISSN 2146-586X

Synthesis, Characterization, And Thermal Conductivity Properties of Graphene Oxide Doped Chromium-Titanium Oxide Structures

Serhat KOÇYİĞİT[1,*]

[1]*Bingol University, Central Laboratory Application and Research Centre, 12000, Bingol, Turkiye*
skocyigit@bingol.edu.tr, ORCID: 0000-0003-0172-6180

Received: 10.10.2024 **Accepted:** 28.11.2024 **Published:** 31.12.2024

Abstract

This study investigates synthesis and characterization of graphene oxide (GO) undoped and doped chromium-titanium oxide structures, along with their thermal conductivity properties in detail. The importance of low or high thermal conductivity varies depending on the intended application, and it is known that thermal conductivity, which determines which determines a material's ability to conduct heat, plays a crucial role in energy, electronics, and thermoelectric applications. Materials with low thermal conductivity are widely used in various industrial fields due to their effective heat insulation capabilities. For experimental studies, GO-undoped(T1), 1%-GO-doped(T2), and 3%-GO-doped(T3) samples were produced via the sol-gel method, followed by calcination, pelletization, and sintering processes. Characterization of these pellets was performed using X-ray Diffraction (XRD), Scanning Electron Microscopy (SEM), and Fourier Transform-Infrared Spectroscopy (FTIR). Thermal conductivity was measured using Physical Properties Measurement System (PPMS). No structural or peak changes were detected in the XRD and FTIR results, but differences in peak intensities were observed. SEM images revealed reductions in structural dimensions with GO doping, which corresponded to changes in thermal conductivity data. The thermal conductivity values of the T1, T2, and T3 samples were measured

* Corresponding Author DOI: 10.37094/adyujsci.1564392

as 6.49, 3.45, and 1.50 W/K·m, respectively. These findings indicate that GO-doping reduces thermal conductivity and that differences in the material structure are significant. Additionally, it was observed that reducing the structure to the nanoscale also led to a decrease in thermal conductivity. These materials could play an important role in developing next-generation material designs.

Keywords: Chrome oxide; Graphene oxide; Sol-gel; Thermal conductivity; Titanium oxide.

Grafen Oksit Katkılı Krom-Titanyum Oksit Yapılarının Sentezi, Karakterizasyonu ve Termal İletkenlik Özellikleri

Öz

Bu çalışmada, grafen oksit katkılı ve katkısız krom titanyum oksit yapılarının sentez ve karakterizasyonları ile birlikte termal iletkenlik özellikleri detaylı bir şekilde incelenmiştir. Termal iletkenlik değerlerinin düşük veya yüksek olması hedeflenen malzeme türüne göre önem arz etmekte ve malzemelerin ısıyı iletme yeteneğini belirleyen termal iletkenliğin enerji, elektronik ve termoelektrik uygulamalarda önemli rol oynadığı bilinmektedir. Düşük termal iletkenliğe sahip malzemeler, ısıyı etkin bir şekilde izole edebilme yetenekleri sayesinde çeşitli endüstriyel alanlarda yaygın olarak kullanılmaktadır. Deneysel çalışmalar sonucunda, GO-undoped (T1), 1% GO-doped (T2) ve 3% GO-doped (T3) örnekleri sol-jel yöntemi ile üretilmiş olup örneklerin ilk olarak kalsinasyonu ardından peletleme sonrası sinterleme işlemi yapılmıştır. Bu sinterlenen peletlerin karakterizasyonu X-ışınları Kırınımı (XRD), Taramalı Elektron Mikroskobu (SEM) ve Fourier Dönüşümlü Kızılötesi Spektroskopi (FTIR) ile yapılmıştır. Termal iletkenlik ölçümleri ise Fiziksel Özellikler Ölçüm Sistemi (PPMS) ile yapılmıştır. Karakterizasyonlarda XRD ve FTIR sonuçlarında herhangi yapı ve pik değişikliği saptanmamış, ancak pik şiddetlerinde farklılıklar görülmüştür. SEM görüntülerinde GO katkılaması ile yapı boyutlarında azalmalar meydana geldiği anlaşılmış ve termal iletkenlik verilerindeki değişimle bu durum açıklanmıştır. T1, T2, ve T3 örneklerinin termal iletkenlik değerleri sırasıyla 6.49, 3.45 ve 1.50 W/K·m olarak ölçülmüştür. Bu bulgular, grafen oksit katkısının termal iletkenliği azalttığını ve malzeme yapısındaki değişikliklerin bu süreçte etkili olduğunu göstermektedir. Ayrıca yapının nanoboyuta indirgenmesiyle termal iletkenlik verilerinin de düştüğü gözlemlenmiştir. Enerji verimliliğini artırma potansiyeli açısından bu malzemelerin yeni nesil malzeme tasarımlarının geliştirilmesinde önemli rol oynayabilecektir.

Anahtar Kelimeler: Krom oksit; Grafen oksit; Sol-jel; Termal iletkenlik; Titanyum oksit.

1. Introduction

Thermal conductivity is a crucial property that determines the heat transfer ability of materials, significantly impacting energy, electronic, and thermoelectric applications [1]. While high thermal conductivity is advantageous in some contexts, low thermal conductivity is beneficial in others. Materials with low thermal conductivity are used in various industrial applications due to their effective heat isolation capabilities. Specifically, metal oxide materials with low thermal conductivity are preferred for use as thermal insulation materials in the construction sector, for controlling heat distribution in electronic circuit systems, for increasing energy efficiency in solar panels, for achieving more precise measurements in heat sensors, and for retaining heat generated from temperature differences in thermoelectric materials [2-4].

The synthesis of nanostructured materials is of great importance due to their higher surface area, higher sinterability, and improved optical, electronic, and magnetic properties [5-7]. Additionally, the increased potential for thermoelectric power generation and the wide thermal management of nanoparticles through phonon transport provide significant advantages in using these structures [8-10].

Chromium oxide nanoparticles are a preferred material due to their ease of synthesis [11]. They offer advantages in doping and possess properties such as durability in high-temperature and high-pressure applications, high wear and corrosion resistance, and catalytic capabilities [12].

Titanium oxide structures can provide thermal insulation due to their low thermal conductivity. Particularly in TiOx structures, it has been observed that the thermal conductivity values decrease as the x value decreases from 2 to 1, with accompanying changes in crystal structures. It is known that even when the x value is between 2 and 1.66, the compound exhibits n-type semiconductor properties, behaves as a p-type semiconductor at room temperature between 1.66 and 1.25, and shows n-type characteristics at room temperature and p-type at higher temperatures when the x value is between 1 and 1.25 [13]. This property allows titanium oxide structures to yield significant results when used in a controlled manner in thermal conductivity data.

Graphene exhibits high thermal conductivity when utilized in its pure, single-layer form, complemented by its exceptional mechanical properties and lightweight nature. While graphene oxide does not match graphene's thermal conductivity levels, the low thermal conductivity of graphene oxide is primarily due to increased phonon-boundary scattering caused by surface functional groups. Since graphene oxide is dispersible in water and organic solvents, it can be used for specific applications [14,15]. Additionally, the structural properties and atomic

interactions with the materials to which it is added can lead to significant reductions in thermal conductivity values [16,17]. Furthermore, the high surface area and nanostructure of graphene oxide significantly influence its thermal conductivity [2]. For instance, graphene and graphene oxide doping have been shown to reduce the potential barrier and grain boundary resistivity by creating high-density oxygen vacancies in SrTiO3 significantly reducing the average grain size, increasing phonon scattering, and thus reducing thermal conductivity [18,19].

This study focuses on the synthesis and characterization of graphene oxide (GO) doped chromium-titanium oxide structures and the effects of varying GO concentrations on thermal conductivity. The findings reveal significant decreases in thermal conductivity with GO doping, providing new insights into the structural changes that affect heat transfer properties at the nanometer scale.

The motivation for this research stems from the increasing demand for materials with specialized thermal properties for applications in energy efficiency, electronics, and thermoelectric systems. As industries increasingly seek materials that can effectively manage heat transfer, it becomes important to understand how additives such as graphene oxide can influence thermal conductivity. This study aims to contribute to the development of next-generation materials that improve energy efficiency and thermal management by addressing both environmental sustainability and technological advancement.

2. Materials and Methods

2.1. Material

In the formation of chromium-titanium oxide, organic salts of these metals were preferred. Chromium (III) acetylacetonate and titanyl acetylacetonate salts were supplied by Sigma-Aldrich. Glacial acetic acid, supplied by Merck, was used to support the solutions of these salts. Graphene oxide, which is >99% pure and in powder form, was supplied by Graphene Supermarket. Polyvinyl alcohol (PVA) (Mw: 85,000 - 124,000) was chosen as the polymer source and was supplied by Sigma-Aldrich.

2.2. Sample preparation

The preparation of chromium-titanium oxide structures began by dissolving the acetate salts of these metals in a water and acetic acid mixture for 6 hours at room temperature using a magnetic stirrer at 250 rpm. 10% (w/v) PVA solution was then dissolved by maintaining a constant temperature of 80 °C for 2 hours, and this solution was left to cool to room temperature [20]. In preparing the graphene oxide dispersion, graphene oxide powder was added to the metal

acetate solution and kept in an ultrasonic bath for 24 hours until the dispersion was ready. The PVA solution was added to the graphene oxide-doped metal acetate mixture and stirred with a magnetic stirrer for 3 hours. Thus, graphene oxide-doped and undoped metal acetate/PVA solutions were prepared. In these mixtures, the graphene oxide undoped was named T1, the 1% graphene oxide-doped was named T2, and the 3% graphene oxide-doped was named T3. To ensure gelation in the prepared T1, T2, and T3 sol-gel mixtures, these mixtures were transferred to porcelain crucibles and dried in an oven at 100 °C. The dried mixtures were then heated in the oven at 650 °C for 4 hours, undergoing a calcination process to remove organic structures. After calcination, the nanomaterials obtained were pulverized in an agate mortar. These powders were then pressed into pellets with a diameter of 8 mm and a thickness of 3 mm under 6 tons of pressure and sent back to the tubular oven, where they were sintered at 850 °C for 4 hours to ensure the fusion of nanoparticles in the material.

2.3. Characterization

The sintered pellet structures were first characterized using XRD, SEM and FTIR, and their thermal conductivities depending on temperature were calculated using a PPMS device. XRD characterization was performed with a PANalytical Empyrean device to create the diffraction pattern of the crystal structures of the sintered pellets. A Zeiss Supra 40VP SEM device was used to reveal the morphological properties of the pellets. The bond structures were analyzed using a PerkinElmer Spectrum 100 Series FTIR spectrometer, which revealed the various vibrational structures of the molecules. A Quantum Design PPMS instrument was used to determine the thermal properties of the samples as a function of temperature. The analyses with the XRD, SEM, and FTIR devices were conducted at Bilecik Şeyh Edebali University, while the PPMS analyses were conducted at Malatya Inönü University.

3. Results and Discussion

3.1. XRD Results

The diffraction patterns of the peak intensities corresponding to the 2θ (two theta) angles of the T1 (black), T2 (red), and T3 (blue) samples, obtained from X-ray diffraction (XRD) analysis, are presented in Fig. 1. Upon examining the XRD diffraction patterns, it was observed that all samples contained two crystal structures and exhibited the same peak values. Analysis of these peak values indicated that they corresponded to the peaks of the Cr_2O_3 compound, which has a rhombohedral crystal structure, as referenced by the Joint Committee on Powder Diffraction Standards (JCPDS) # 00-038-1479 [21]. It was determined that the 2θ values of the rhombohedral Cr_2O_3 peaks were at 36.71°, 42.60°, and 61.83°, with orientations of (111), (002), and (022),

respectively. Additionally, it was found that the peaks also belonged to the Ti_1O_1 compound, which has a cubic crystal structure, as referenced by JCPDS # 98-005-6612 [22]. The cubic crystal structure Ti_1O_1 peaks were identified at 24.52°, 33.63°, 34.27°, 41.53°, 50.33°, 54.95°, and 63.58°, with orientations of (012), (104), (110), (113), (024), (116), and (214), respectively. Due to the low concentrations of graphene oxide doping, at 1% and 3%, these peaks were not observed in the XRD diffraction patterns. No structural change was deteted as a result of graphene oxide doping; only differences in peak intensities were noted. This indicates that no degradation occurred in the structure due to graphene oxide doping. The results in the diffraction pattern also confirm the compound structure.

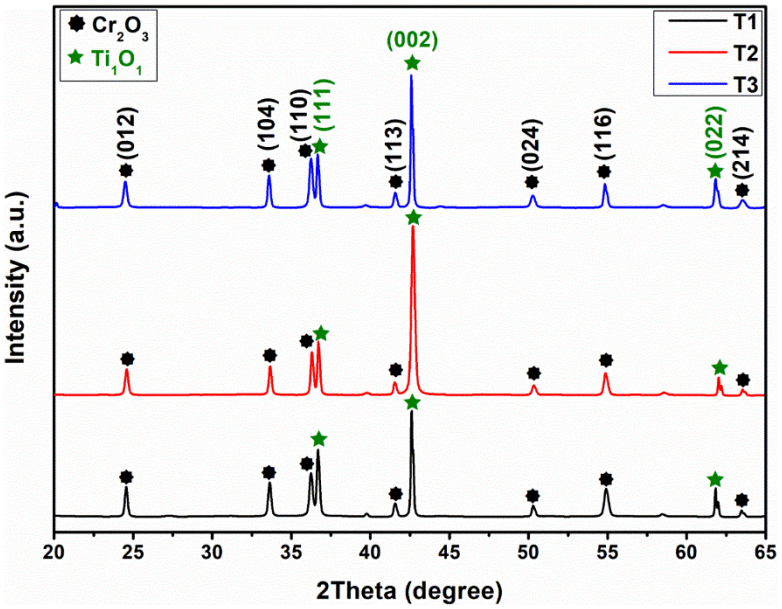

Figure 1: X-ray diffraction pattern of T1 (black), T2 (red), and T3 (blue) samples.

3.2. SEM Results

SEM images of the T1, T2, and T3 samples are presented in Figure 2. These images were captured at a voltage of 15 kV and magnification of 100,000x. Upon examining the SEM images, a comparison of the T1 and T2 samples reveals that they exhibit similar structures. However, it is evident that the gap ratio between the structures in the T2 sample is greater than that in the T1 sample, and the clusters are denser. While the T1 and T2 samples exhibit similar clustering, the T3 sample shows that the nanostructures are detached from the clustered formations, resulting in a reduction of the average diameter of the structures. Measurements indicated that the diameters of the clustered structures in the T1 sample ranged from 60 to 80 nm, while those in the T2 sample varied between 60 and 110 nm. In contrast, the diameters of the separated structures in the T3 sample were found to range from 20 to 40 nm.

Goncalves et al. stated that higher-density oxygen functional groups support the dispersion of nanoparticles along the graphene oxide surface and suggested that oxygen groups on the GO surface affect the size growth of nanoparticles [23]. Thus, it was observed that there were openings between the particles and the particles grew due to the effect of oxygen groups in the T1 and T2 samples. While there was a particle cluster where the particles merged in the T1 and T2 samples, it is estimated that in the T3 sample, due to this feature of GO, the particle cluster opened and the particles inside were separated. It was understood that the particle size decreased due to the size of the opened particles.

Given that it is established that thermal conductivity decreases with reduced phonon participation in nanotechnological processes and increased gaps between structures, it can be concluded that the temperature-dependent thermal conductivity data presented in Fig. 4 is consistent with the SEM images.

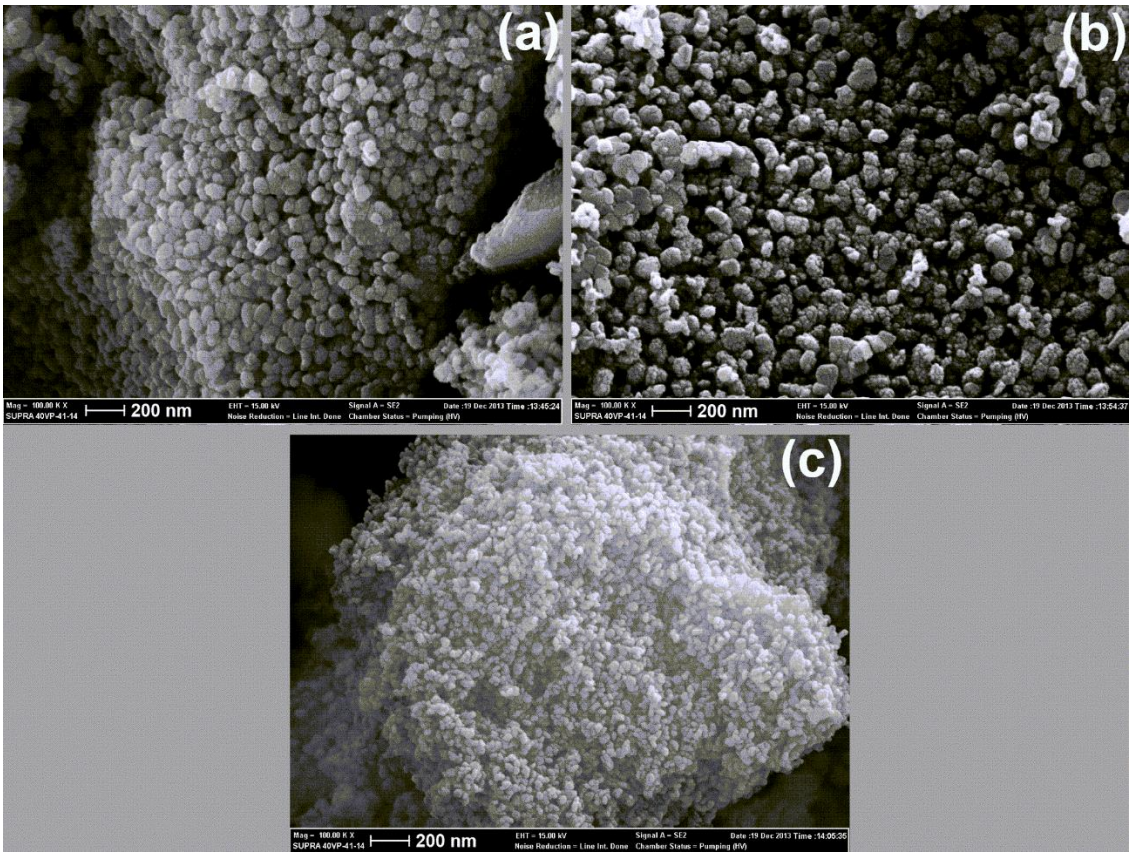

Figure 2: SEM images of T1 (a), T2 (b), and T3 (c) samples (15 kV, 100000x).

3.3. FTIR Results

The FTIR spectra for the T1, T2, and T3 calcined powder samples are illustrated in Figure 3. Analyzing this graph reveals that all samples display identical peak structures, suggesting that

their molecular compositions are also the same. Specifically, the peaks observed at 2162 cm^{-1}, 1971 cm^{-1}, and 1625 cm^{-1} are recognized as corresponding to Cr2O3, as supported by previous studies [24,25]. Furthermore, the peaks located at 907 cm^{-1}, 872 cm^{-1}, and 763 cm^{-1} align with the Ti-O-Ti structural configuration, indicating the presence of titanium oxide in the samples [26]. The peaks at 606 cm^{-1} and 479 cm^{-1} have been identified as compatible with Cr-O bonds, further confirming the presence of chromium oxide in the structures. Additionally, the peak at 424 cm^{-1} is found to overlap with titania structures, reinforcing the structural integrity of the materials [27]. Due to the low concentrations of graphene oxide doping, at 1% and 3%, these peaks were not observed in the FTIR spectra. These findings suggest that the presence of both Ti-O and Cr-O structures in the FTIR spectra aligns with the results obtained from the XRD diffraction patterns. This correlation between the two characterization techniques provides strong evidence that they validate each other, enhancing the reliability of the analysis conducted on these samples.

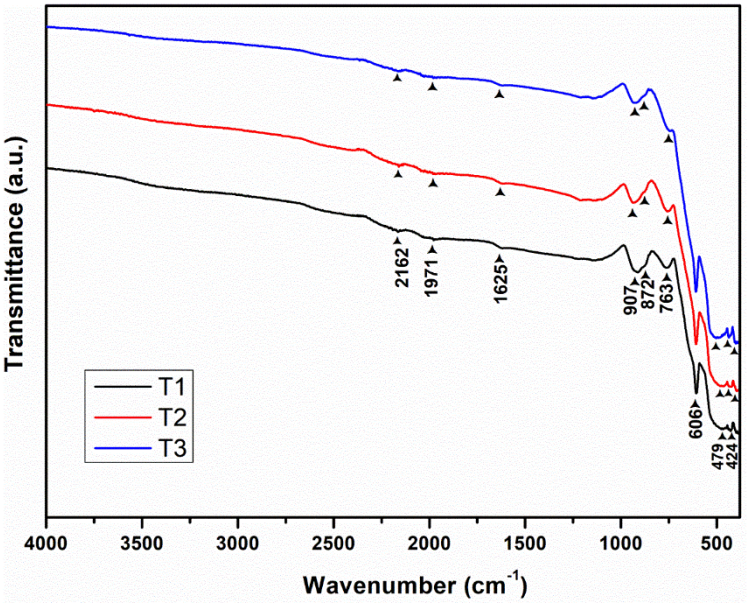

Figure 3: FTIR spectra of T1 (black), T2 (red), and T3 (blue) samples.

3.4. Thermal Conductivity Results

When examining the thermal conductivity versus temperature values of the T1, T2, and T3 samples, it was determined that the thermal conductivity value ranking for each temperature is T1 > T2 > T3, as shown in Figure 4. This ranking is related to the structural properties of the materials and the effects of dopants. Notably, when the graphene oxide content is 1%, a slight decrease in thermal conductivity is observed. Increasing the graphene oxide content to 3% further reduces the thermal conductivity value.

Upon examining the SEM images, it was observed that in the graphene oxide undoped sample, the nanostructures are clustered. In the 1% graphene oxide doped sample, similar clustering was detected; however, in this case, the clustered structures were observed to be separated from each other. This formation of voids has contributed to the decrease in thermal conductivity. In the T3 sample, it was found that the clustered structures in the T1 and T2 samples were completely separated. In this sample, the structure demonstrates more pronounced nanoproperties, and this observation is further supported by the particle size data derived from the SEM images.

The thermal conductivity values for the T1, T2, and T3 samples, measured at room temperature (298 K), were found to be 6.49, 3.45, and 1.50 W/K·m, respectively. In this context, the effect of graphene oxide as a dopant in reducing thermal conductivity is related to changes in the material structure, indicating that phonon activity plays a significant role in the thermal management of nanostructured materials [9,28,29].

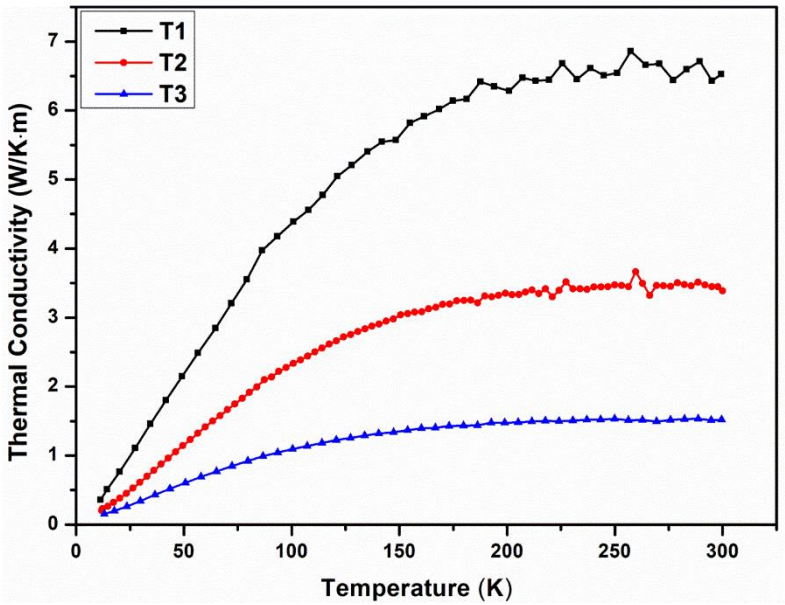

Figure 4: Thermal conductivity vs temperature graphs of T1 (black), T2 (red), and T3 (blue) samples.

This study aims to provide innovative solutions to increase energy efficiency and control heat through the combination of materials used. This approach could serve as an important foundation for the development of next-generation material designs and the improvement of existing applications, with positive effects on energy savings, heat management, and environmental sustainability**.**

4. Conclusion

In this study, the synthesis, characterization, and thermal conductivity properties of graphene oxide-doped and undoped chromium-titanium oxide structures were investigated in detail. The findings show that graphene oxide doping significantly reduces thermal conductivity. Thermal conductivity values of the T1, T2, and T3 samples were measured as 6.49, 3.45, and 1.50 W/K·m at room temperature, respectively. These results reveal the effects of graphene oxide on thermal conductivity along with the changes it induces in the material structure.

X-ray diffraction (XRD) and Fourier transform infrared spectroscopy (FTIR) analyses confirmed that all samples have similar molecular structures, and no structural changes were observed. Scanning electron microscope (SEM) images showed that graphene oxide doping causes expansion in the structure with the increase in the presence of oxygen in structural dimensions, which is related to thermal conductivity data.

In conclusion, graphene oxide-doped chromium-titanium oxide structures can play an important role in the development of new-generation material designs due to their potential to increase energy efficiency. The effects of these materials on thermal management applications and environmental sustainability provide an inspiring basis for future research.

References

[1] Tritt, T.M., *Thermal conductivity: Theory, properties, and applications:* Springer Science & Business Media, 2005.

[2] Eivari, H.A., Sohbatzadeh, Z., Mele, P., Assadi, M.H.N., *Low thermal conductivity: Fundamentals and theoretical aspects in thermoelectric applications*, Materials Today Energy, 21, 100744, 2021.

[3] Binici, H., Aksogan, O., Demirhan, C., *Mechanical, thermal and acoustical characterizations of an insulation composite made of bio-based materials*, Sustainable Cities and Society, 20, 17-26, 2016.

[4] Tsilingiris, P.T., *Heat transfer analysis of low thermal conductivity solar energy absorbers*, Applied Thermal Engineering, 20, 1297-1314, 2000.

[5] Chavan, S.V., Sastry, P.U.M., Tyagi, A.K., *Combustion synthesis of nanocrystalline Nd-doped ceria and Nd_2O_3 and their fractal behavior as studied by small angle X-ray scattering*, Journal of Alloys and Compounds, 456, 51–56, 2008.

[6] Gleiter, H., *Nanocrystalline solids*, Journal of Applied Crystallography, 24, 79-90, 1991.

[7] Weller, H., *Colloidal semiconductor q-particles-chemistry in the transition region between solid-state and molecules*, Angewandte Chemie International Edition in English, 32, 41–53, 1993.

[8] Narayanamurti, V., *Phonon optics and phonon propagation in semiconductors*, Science, 213, 717-723, 1981.

[9] Maldovan, M., *Phonon wave interference and thermal bandgap materials*, Nature Materials, 14, 667-674, 2015.

[10] Xie, G., Ding, D., Zhang, G., *Phonon coherence and its effect on thermal conductivity of nanostructures*, Advances in Physics: X, 3, 720-755, 2018.

[11] Liu, G., Liu, Z., Wang, L., Zhang, K., Xie, X., *A combined chrome oxide and titanium oxide based electron-transport layer for high-performance perovskite solar cells*, Chemical Physics Letters, 771, 138496, 2021.

[12] Pei, Z., Zheng, X., Li, Z., *Progress on synthesis and applications of Cr_2O_3 nanoparticles*, Journal of Nanoscience and Nanotechnology, 16, 4655-4671, 2016.

[13] He, Q., Hao, Q., Chen, G., Poudel, B., Wang, X., Wang, D., Ren, Z., *Thermoelectric property studies on bulk TiO_x with x from 1 to 2*, Applied Physics Letters, 91, 052505, 2007.

[14] Pei, Q.X., Sha, Z.D., Zhang, Y.W., *A theoretical analysis of the thermal conductivity of hydrogenated graphene*, Carbon, 49, 4752-4759, 2011.

[15] Chen, J., Li, L., *Thermal conductivity of graphene oxide: a molecular dynamics study*, JETP Letters, 112, 117-121, 2020.

[16] Chen, J., Li, L., *Thermal conductivity of graphene oxide: A molecular dynamics study*, JETP Letters, 112, 117-121, 2020.

[17] Sevinçli, H., Sevik, C., Çağın, T., Cuniberti, G., *A bottom-up route to enhance thermoelectric figures of merit in graphene nanoribbons*, Scientific Reports, 3, 1228, 2013.

[18] Huang, J., Yan, P., Liu, Y., Xing, J., Gu, H., Fan, Y., Jiang, W., *Simultaneously breaking the double Schottky barrier and phonon transport in $SrTiO_3$-based thermoelectric ceramics via two-step reduction*, ACS Applied Materials & Interfaces, 12, 52721-52730, 2020.

[19] Liu, X., Li, S., Yu, J., Zhu, Y., Lin, K., Wang, B., Rongsheng, C., Dursun, E., David L., Ian, A.K., Michael J.R., Freer, R., *Enhancing the thermoelectric properties of TiO_2-based ceramics through addition of carbon black and graphene oxide*, Carbon, 216, 118509, 2024.

[20] Koçyiğit, S., Aytimur, A., & Uslu, I., *Graphene-doped $Ca_{0.9}Er_{0.1}Mn_{1.5}O_\alpha$ thermoelectric nanocomposite materials: Temperature-dependent thermal and Seebeck properties*, Ceramics International, 46, 6377-6382, 2020.

[21] Yue, H.R., Xue, X.X., Zhang, W.J., *Diffusion Characteristics of Intermediate in Cr_2O_3/CaO System and Its Formation Mechanism*, Metallurgical and Materials Transactions B, 52, 3477-3489, 2021.

[22] Filiberto, M., Daniele, B., Franco, B., Antonio, S., Adriano, P., Giovanna, I., Raimondo, Q., *Histological and histomorphometric comparison of innovative dental implants laser obtained: Animal pilot study*, Materials, 14, 1830, 2021.

[23] Goncalves, G., Marques, P.A., Granadeiro, C.M., Nogueira, H.I., Singh, M.K., Gracio, J., *Surface modification of graphene nanosheets with gold nanoparticles: the role of oxygen moieties at graphene surface on gold nucleation and growth*, Chemistry of Materials, 21, 4796-4802, 2009.

[24] Hallam, H.E., *Infrared and Raman spectra of inorganic compounds*, Royal Institute of Chemistry, Reviews, 1, 39-61, 1968.

[25] Scarano, D., Zecchina, A., Bordiga, S., Ricchiardi, G., Spoto, G., *Interaction of CO with α-Cr_2O_3 surface: A FTIR and HRTEM study*, Chemical Physics, 177, 547-560, 1993.

[26] Nakamura, R., Nakato, Y., *Primary intermediates of oxygen photoevolution reaction on TiO_2 (rutile) particles, revealed by in situ FTIR absorption and photoluminescence measurements*, Journal of the American Chemical Society, 126, 1290-1298, 2004.

[27] Kumar, P.M., Badrinarayanan, S., Sastry, M., *Nanocrystalline TiO_2 studied by optical, FTIR and X-ray photoelectron spectroscopy: correlation to presence of surface states*, Thin solid films, 358, 122-130, 2000.

[28] Mahanta, N.K., Abramson, A.R., *Thermal conductivity of graphene and graphene oxide nanoplatelets*, 13th InterSociety Conference on Thermal and Thermomechanical Phenomena in Electronic Systems, 1-6, 2012.

[29] Okhay, O., Tkach, A., *Impact of graphene or reduced graphene oxide on performance of thermoelectric composites*, Journal of Carbon Research, 7, 37, 2021.